JMEPEG (2011) 20:257–264
DOI: 10.1007/s11665-010-9669-2

1059-9495/$19.00

Analysis of Heat Effects on Marine Corps AM2 Mat Mechanical Properties

V. Vega, U. Nguyen Huynh, J. Holmes, J. DeChellis, P. Stoyanov, D. Piatkowski, E.W. Lee, J. Ogren, N. Drusina, and O.S. Es-Said

(Submitted October 2, 2009; in revised form January 29, 2010)

Navy AM2 mats are used as portable aircraft landing platforms for the Short Take-off/Vertical Landing (STOVL) aircraft operations. This investigation presents the study performed to determine whether the surface discoloration is a precursor to degradation in the mechanical property of the AM2 mat material. The red discoloration on the mat surfaces had a clear correlation with the decrease in yield strength, ultimate strength, and hardness properties.

Keywords AM2 mats, STOVL, 6061-T6 aluminum

1. Introduction

Temporary airfield landing surfaces composed of hollow plates of Al 6061-T6 alloy are known as AM2 mats (Ref 1-3). The mats that are exposed to the Short Take-Off/Vertical Landing (STOVL) aircraft exhibited surface discoloration. Two AM2 portable mats (identified as Mat C and Mat D) with visible signs of discoloration were used for this investigation. The surface discoloration results from exhaust exposure reaching high temperatures of 700 °C (1300 °F). This temperature may degrade the mechanical properties of the aluminum alloy mats, even for short temperature exposure durations (Ref 1). These mats were used during the evaluation of the STOVL aircraft during the initial stages of the aircraft development. There was no clear accounting for the number of times, or even regarding whether, the aircraft actually performed vertical takeoffs or landings on those particular mats. The damage, most likely, is due to the aborted attempts to take off vertically. An aborted attempt would consist of the aircraft applying thrust to the engines, but due to some reason not achieving lift. The relationship between these two mats in the airfield structure is also not known, nor is the location of the aircraft on those mats. The study was effective in showing that there is great potential for damage to the mats from this aircraft, a fact that was not known or its extent realized at the time when the aircraft was in its early stage of development. The objective of this study is to correlate the discoloration of the mat surfaces to the mechanical and electrical conductivity properties.

V. Vega, Northrop Grumman Corporation, Operations Analysis, One Hornet Way, El Segundo, CA 90425; **U. Nguyen Huynh, J. Holmes, J. DeChellis, P. Stoyanov, J. Ogren,** and **O.S. Es-Said**, Mechanical Engineering Department, Loyola Marymount University, Los Angeles, CA 90045-8145; **D. Piatkowski**, Naval Air Systems Command, Naval Air Warfare Center, Aircraft Division, Lakehurst, NJ 08733-5083; **E.W. Lee**, Naval Air Systems Command, Naval Air Warfare Center, Patuxent River, MD 20670-1908; and **N. Drusina**, Nortrop Grumman Corporation, Materials Engineering, One Space Park, Redondo Beach, CA 90278. Contact e-mail: oessaid@lmu.edu.

2. Experimental

2.1 Material

AM2 mats are composed of extruded aluminum alloy, 6061-T6. The typical chemical composition and mechanical properties are shown in Table 1 and 2, respectively. The AM2 mats are constructed with vertical spars running parallel to the direction of extrusion. Integral connectors are welded at each end of the mat perpendicular to the spars (Ref 1). These mats are assembled into a brickwork-like pattern to form runways, parking areas, and taxiways for battlefield aircraft operations. The dimensions of each mat are 356 cm by 61 cm by 3.8 cm (144 by 24 by 1.5 in.), and each mat weighs about 65.3 kg (144 lbs.). The surfaces are also coated with a non-skid epoxy coating.

2.2 Machining and Labeling Procedure

Fourteen sections were machined, 25.4 by 61.0 cm (10 by 24 in.), perpendicular to the length of each of the AM2 mats. These sections were cut into bars of 2.54 by 25.4 cm (1 by 10 in.), and then milled into tensile samples of 0.64 cm (0.25 in.) in thickness as shown in Fig. 1.

The tensile samples (quantity of 475) were machined parallel to the direction of the internal vertical spars (longitudinal), and 20 transverse tensile samples were machined in the perpendicular direction. The longitudinal samples were tested for tensile strength, hardness, and electrical conductivity. The electrical conductivity tests were performed first, and hardness values were taken at the grips. The transverse samples were only tensile and hardness tested. The non-skid coating on the mat surface was removed (by milling) to avoid any inconsistencies in the amount of percent elongation in the final tensile testing. Also the bow-shaped undersurfaces of the bars taken from the top of the mats were milled flat (Ref 1).

Table 1 Chemical composition of 6061 aluminum alloy (Ref 4, 5)

Al 6061-T6	Al	Cr	Cu	Fe	Mg	Mn	Si	Ti	Zn
wt.%	98	0.04-0.35	0.15-0.4	0.7	0.8-1.2	0.15	0.4-0.8	0.15	0.25

Table 2 Minimum standard material properties of 6061-T6 aluminum alloy (Ref 4, 5)

Ultimate strength, MPa (ksi)	Yield strength, MPa (ksi)	%Elongation	Hardness (15T) min.	Conductivity
290 (42)	241 (35)	10	80 (a)	40% IACS (a)

(a) Typical values

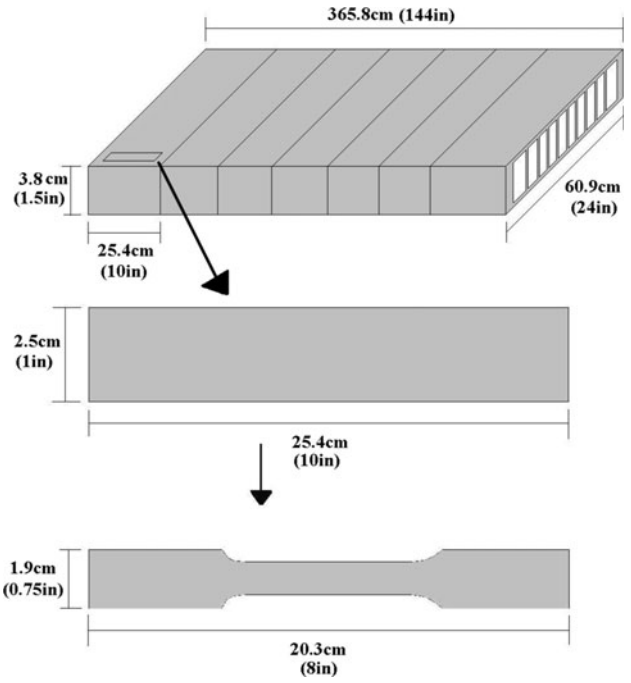

Fig. 1 Step-by-step illustration of the milling process

2.3 Testing Procedure

Tensile testing was performed using an Instron 4505 universal testing machine, conductivity was tested using a Hocking Auto Sigma 3000 tester, and hardness was determined with the superficial Rockwell 15T scale tester.

3. Results

The data were collected to generate rough color contour maps. Each cell in the contour maps represents the actual position of the sample on the mats. The numbers from 1 through 14 on top and from 1 through 13 on the left of the contour map represents the location of the sample on each mat, Fig. 2-6. The black cells are the samples that were not tested. The remaining cells with numbers represent the tested samples with their corresponding values according to each test. Above each contour map is an actual photograph of the AM2 mats used for this investigation. The top section is shown above, and the bottom section is shown below it. These photographs demonstrate the effects of heat exposure on the aluminum 6061-T6's mats. The AMS mechanical property standards were used to evaluate the results of Mat C and Mat D, see Table 2.

3.1 Mat C

The following results describe the mechanical properties for Mat C in regard to the materials yield strength, ultimate tensile strength, hardness, and electrical conductivity. The results were shaded and grouped to show a distinction in the properties of the mat.

Figure 2(a) shows the yield strength results of Mat C. The top of Mat C shows the lowest yield strength values on the left-side portion of the mat. The average value of the lowest grouping (horizontal lines) is 248 MPa (standard deviation of 3.9) which still exceeds the yield strength minimum 220.5 MPa (32 ksi). The averages of the vertical and downward diagonal lines areas are 267 and 286 MPa (standard deviations of 5.2 and 4.6), respectively. Figure 2(b) shows the contour plot of the yield strength from column 1 through column 8 of the top mat. The contour plot shows no apparent difference in the yield strength values. The bottom section of the mat was less affected. This is expected because the top of the mat is directly exposed to the high temperature exhaust gases. The lower values correspond to the discoloration of the mat itself.

Figure 3(a) shows the ultimate strength results of Mat C. The bottom of the mat again is less affected as compared to the top of the mat. The portions corresponding to the discoloration in the mat has lower values than the minimum standard (Ref 4), Table 2. The average value of this section (vertical lines) was 271 MPa (standard deviation of 2.7). Several portions have values between 261.8 and 289.4 MPa (38-42 ksi) in the top of the mat, while only few portions have similar lower values at the bottom of the mat. Figure 3(b) shows the ultimate strength values from column 1 through 8 of the top mat as a contour plot. The variation of ultimate strength values of the mat is more apparent in this contour plot as compared to the yield strength values in Fig. 2(b).

Figure 4(a) shows the hardness results of Mat C. While the top of the mat shows a decrease in hardness correlating to the discoloration on the mat photograph, the bottom does not show a change in hardness. Some portions corresponding to the discoloration of the mat have lower values of hardness as compared to the typical values, Table 2.

Figure 5(a) shows the electrical conductivity of Mat C. All values are above the typical value. Those high electrical conductivity values indicate that the mat is not as strong as it was before being put into use. However, there is no correlation between the discoloration of the mat and the electrical conductivity values of Mat C since the results are uniform throughout the mat.

Contour plots for the hardness and conductivity of Mat C can be seen in Fig. 4(b) and 5(b), again from column 1 though column 8 of the top mat. The most affected area for the hardness in Mat C (horizontal lines) has an average value of 79 (standard deviation of 0.74) while the most affected area for the conductivity of Mat C (vertical lines) is 46.5 (standard deviation of 0.06).

Mat C

	1	2	3	4	5	6	7	8	9	10	11	12	13	14
13					290.8	287.3					285.9		288.7	
12	294.9	294.9	286.6	285.2	286.6	288.7	285.2	291.4	296.3	297.0		297.0		295.6
11	286.6	285.9	283.2	279.0	291.4	287.3		294.2						
10		288.0	285.2	285.2	290.8	286.6	284.6		299.7	297.6	294.2	290.1	292.8	290.8
9	286.6	305.2	278.4	279.0	284.6	279.7	281.8	294.9						
8	288.0	283.2	280.4	272.8	281.1		290.8		301.8					
7	285.2	279.0	273.5	291.8	266.0	272.8	290.1	292.8		292.1		294.2	292.8	292.8
6	286.6	281.8	273.5	257.0	266.0	272.8	288.7	292.1	300.4					
5		268.0	262.5	245.3	250.8		283.9	285.2						
4	288.0	278.4	259.8	246.0	253.6	271.5	295.6	288.7		299.0	296.3	296.3	299.7	302.5
3	285.2	266.0	249.4	241.2	249.4	268.7	289.4		299.7					
2	289.4	272.2		248.0	254.2	272.8	290.8	293.5	295.6					
1	287.3	265.3	252.2	247.4	261.8	277.7	284.6	293.5	292.1	292.8	286.6	284.6	285.9	

Top Section Results for Mat C

	1	2	3	4	5	6	7	8	9	10	11	12	13	14
13											294.9		281.8	
12	288.7	290.8	295.6		298.3	296.3	286.6	282.5	301.1	293.5		301.1		299.0
11	304.5	306.6	307.3	314.9	304.5	311.4		301.1						
10		294.9	292.8	294.2	297.0	297.6	292.1		293.5	295.6	294.2	295.6	288.0	285.2
9	310.1	311.4	309.4	310.7	310.1	313.5	308.0	310.7						
8	299.0	304.5	302.5		298.3	304.5	301.8		300.4					
7	301.8	303.2	297.0	301.1	303.8	305.2	304.5			303.2	301.8	290.8	304.5	295.6
6	300.4	300.4	299.7	309.4	302.5	304.5	298.3		300.4					
5	303.8	309.4	306.6	308.0	312.1		307.3	312.1						
4	290.1	297.6	292.1		297.0	292.1	299.7	301.1				286.6		281.8
3	303.8	305.9	286.6	303.2	296.3	304.5	300.4		299.7					
2	293.5	290.1	314.2	293.5	306.6	292.1	309.4	298.3						
1	296.3	281.1	285.9	254.9	288.7	295.6	301.1	283.2	292.1		295.6	294.2	300.4	292.8

Bottom Section Results for Mat C

(a)

≤ 254.9
255 – 275.9
276 – 295.9
296-316.9
≥ 317
Not Tested

(b)

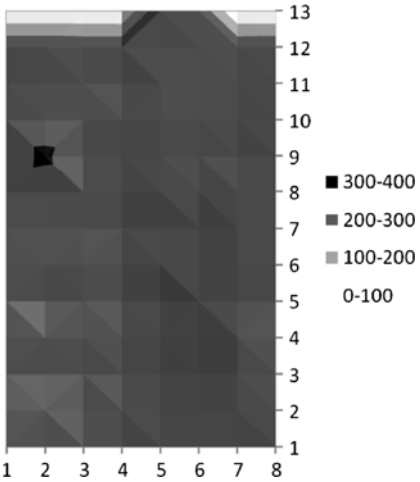

Fig. 2 (a) Yield strength of Mat C (measured in MPa). (b) Contour plot of yield strength of Mat C (MPa)

Mat C

	1	2	3	4	5	6	7	8	9	10	11	12	13	14
13					307.3	303.2					303.2		303.8	
12	308.7	308.7	303.8	303.2	304.5	305.9	300.4	307.3	301.8	312.1		309.4		307.3
11	305.9	304.5	303.8	299.7	308.7	306.6		313.5						
10		304.5	301.8	301.1	307.3	305.2	300.4		316.9	305.2	309.4	303.8	301.8	294.2
9	306.6	282.5	298.3	301.8	304.5	302.5	300.4	313.5						
8	301.8	298.3	299.7	292.1	300.4		306.6		310.7					
7	305.2	299.0	297.6	285.9	291.4	294.2	308.7	312.8		302.5		312.1	307.3	305.9
6	301.8	301.1	293.5	279.0	288.7	291.4	305.2	305.9	311.4					
5	303.8	291.4	286.6	272.2	277.7		305.2	305.2						
4	305.2	297.0	280.4	270.1	275.6	292.1	311.4	303.8		312.8	310.1	305.9	313.5	316.3
3	303.2	285.2	274.2	266.0	272.8	284.6	308.0		308.7					
2	303.8	287.3		270.1	277.7	290.8	305.2	308.0	309.4					
1	301.1	281.1	272.2	270.8	282.5	299.7	302.5	309.4	305.2	308.7	301.1	297.0	294.9	

Top Section Results for Mat C

	1	2	3	4	5	6	7	8	9	10	11	12	13	14
13											308.7		288.0	
12	301.8	303.2	301.8	296.3	308.0	306.6	299.0	288.0	312.8	307.3		303.8		303.8
11	323.8	324.5	323.8	318.3	325.2	313.5		316.3						
10		297.6	303.8	309.4	311.4	311.4	303.2		303.2	313.5	301.8	304.5	292.8	291.4
9	328.0	329.3	326.6	332.1	330.0	331.4	326.6	328.7						
8	312.8	316.9	316.3	314.9	310.7	319.7	317.6		313.5					
7	319.7	319.7	303.8	308.7	319.7	318.3	308.7			316.9	309.4	312.1	314.2	303.8
6	312.1	312.8	314.2	316.9	310.7	319.0	310.1		316.9					
5	321.8	321.1	325.2	316.9	328.0		325.2	328.0						
4	301.1	306.6	297.0		311.4	306.6	312.8	313.5		311.4	290.1	296.3	281.8	292.1
3	322.5	321.8	304.5	328.0	319.7	323.8	322.5		315.6					
2	304.5	301.8	326.6	306.6	293.5	307.3	317.6	310.7	293.5					
1	306.6	300.4	299.0	274.2	301.8	312.1	314.9	299.0	309.4		305.9	312.8	305.2	307.3

Bottom Section Results for Mat C

(a)

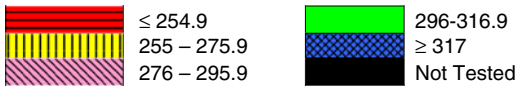

(b)

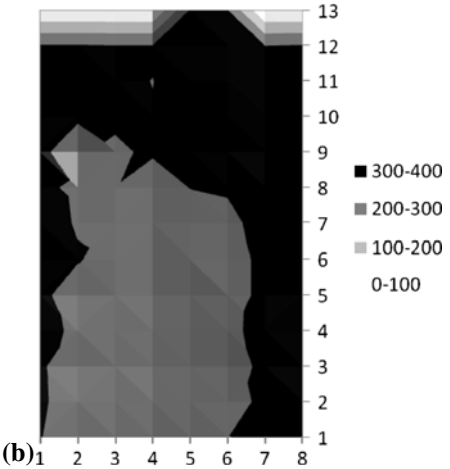

Fig. 3 (a) Ultimate strength of Mat C (measured in MPa). (b) Contour plot of ultimate strength of Mat C (MPa)

Mat C

	1	2	3	4	5	6	7	8	9	10	11	12	13	14
13					81	82					81		82	
12	81	81	81	81	80	82	82	82	82	82				82
11	81	81	81	80	81	82		82						
10		80	81	81	81	81	81		81	81	81	81	82	81
9	80	80	80	80	79	81	81	82						
8	80	81	81	80	80		81		81					
7	80	80	80	78	78	81	81	82		81	81	82	82	82
6	81	80	80	79	79	80	81	81	81					
5	80	80	80	78	79		81	82						
4	81	79	79	78	78	80	81	81		81	81	81	81	81
3	80	80	79	78	78	80	82		81					
2	81	79		78	79	80	81	81	82					
1	80	79	79	79	79	81	80	81	81	81	81	81	80	

Top Section Results for Mat C

	1	2	3	4	5	6	7	8	9	10	11	12	13	14
13				80							81		81	81
12	80	80	81	82	81	83	82	81	82	81		81		
11	81	82	81		81	83		82						
10		82	81	81	81	82	81		82	81	82	80	81	
9	81	81	81	81	81	84	83	82						
8	81	81	81	81	81	83	82		82					
7	81	81	81	81	81	83	82	83		82	83	83	83	
6	81	81	81	81	81	83	82		82					
5	80	81	81	81	81		82	82						
4	81	80	81		81		82	82		82	81	81	84	
3	81	80	81	81	81	82	83	81	81					
2	80	81	81	81	81	82	82	82	82					
1	80		81		80	83	82	81	82		81		82	84

Bottom Section Results for Mat C

(a)

≤ 79
80-81
82-83
84-85
≥ 86
Not Tested

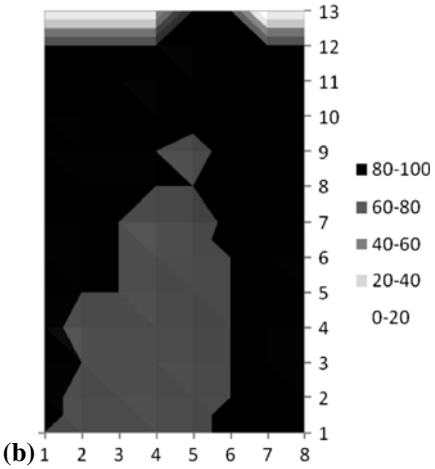

(b)

Fig. 4 (a) Hardness of Mat C (measured on superficial Rockwell 30T scale). (b) Contour plot of hardness of Mat C (measured on superficial Rockwell 30T scale)

Mat C

	1	2	3	4	5	6	7	8	9	10	11	12	13	14
13					47.0	46.8					47.2		47.3	
12	47.2	47.1	47.1	47.2	46.7	47.1	47.2	47.2	47.3	47.4		47.3		47.2
11	46.6	46.6	46.5	46.7	47.3	46.7		46.8						
10		46.8	47.0	47.0	46.9	46.9	47.0		47.3	47.1	47.3	47.3	47.5	47.3
9	46.7	46.5	46.6	46.5	46.6	46.6	46.7	46.7						
8	47.0	46.7	46.7	46.8	46.9		46.7		47.2					
7	46.5	46.4	46.4	46.3	46.4	46.5	46.5	46.6		46.6		46.7	46.8	46.6
6	46.7	46.9	46.9	46.7	46.8	46.8	46.6	46.9	47.1					
5	46.6	46.6	46.4	46.5	46.7	46.5	46.5	46.7						
4	47.0	46.9	47.0	47.0	46.9	46.9	47.0	47.1		47.3	47.3	47.1	47.3	46.9
3	46.6	46.5	46.7	46.6	46.8	46.6	46.8	46.8	46.8					
2	47.2	47.1		47.1	46.4	46.9	47.0	47.0	47.3					
1	47.2	46.6	47.1	47.0	46.5	47.2	47.4	47.4	47.2	47.0	47.2	47.4	47.2	

Top Section Results for Mat C

	1	2	3	4	5	6	7	8	9	10	11	12	13	14
13					46.8	46.9					47.0		47.0	
12	46.9	47.0	46.9	47.0	47.0	47.1	47.0	46.8	47.2	47.3		47.2		47.1
11	46.9	46.8	46.9	46.9	47.0	47.0		46.9						
10		46.9	47.0	47.0	47.1	47.3	47.2		47.4	47.5	47.6	47.6	47.7	47.5
9	46.8	46.8	46.7	46.7	46.8	46.8	46.7	46.8						
8	46.9	46.9	46.9	47.0	47.0	47.0	47.0		47.2					
7	46.7	46.6	46.6	46.6	46.6	46.7	46.6	46.7		46.7	46.8	46.8	46.8	46.7
6	46.9	46.9	46.8	46.9	46.9		47.1		47.3					
5	46.7	46.6	46.6	46.7	46.7		46.6	46.7						
4	46.9	47.0	47.0	46.9	46.9	47.1	47.1	47.1		47.3	47.3	47.5	47.4	47.5
3	47.0	47.0	46.9	46.9	46.9	47.1	47.0	47.0	47.1					
2	46.9	46.9	47.1	47.0	46.9	47.1	47.0	47.2	47.2					
1	46.8	46.7	46.7	46.5	46.9	46.9	46.8	47.0	47.0	46.9	47.0		46.8	46.8

Bottom Section Results for Mat C

(a)

≤ 46.0
46.1 – 46.5
46.6 – 47.0
47.1 – 47.5
≥ 47.6
Not Tested

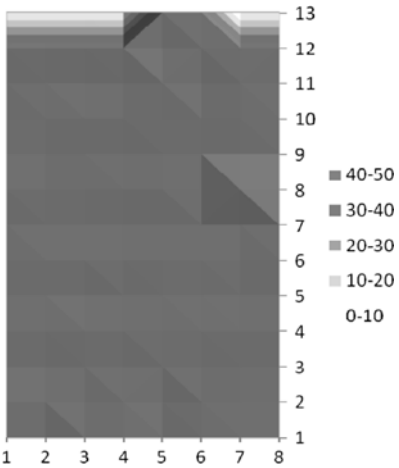

(b)

Fig. 5 (a) Conductivity of Mat C (measured in %IACS). (b) Contour plot of conductivity of Mat C

Mat D

	1	2	3	4	5	6	7	8	9	10	11	12	13	14
13	279.7	287.3	285.2	282.5	283.2	292.8	294.9	297.0						
12	273.5		259.8	268.0	274.2	283.2	287.3	288.7			292.1		291.4	
11	278.4	281.1	261.8	272.2	276.3		292.1	296.3		294.2				292.8
10	279.7	278.4	272.8	277.0	285.9	287.3		288.7	290.8			292.8		
9	283.9	284.6	277.0	285.9	294.2	289.4	297.0	303.2		296.3				
8	285.2	297.0	286.6	289.4	290.8	294.2	296.3	306.6	295.6		298.3			297.0
7	284.6	293.5	294.9	294.2	296.3	297.6	302.5		303.2				297.0	
6	288.0	286.6	289.4	293.5	295.6	294.2	297.6	299.7		292.8		292.8		
5	289.4	293.5	297.6	292.1	294.2	292.1	299.7				297.0			
4	279.7	285.2	288.0	291.4	294.2	293.5	294.9		295.6	292.8				
3	296.3	291.4	295.6	296.3	297.6	297.6		291.4				301.8	298.3	
2	290.1	287.3		297.6	298.3	296.3	299.0	297.0			296.3			298.3
1		289.4	294.9	292.8	294.2	297.0			297.0	290.1				

Top Section Results for Mat D

	1	2	3	4	5	6	7	8	9	10	11	12	13	14
13	266.6	276.3	283.2	274.9	286.6	297.0	297.0	275.6	292.1	281.8				
12	279.0	285.2	287.3	288.7	289.4	291.4	292.1	288.7			291.4		292.1	
11	289.4	285.9	292.8	292.8	294.2	290.8	294.2	288.7		292.8				288.7
10	285.9	288.7	279.7	286.6	293.5	292.8	297.0	290.8	293.5			291.4		
9	321.8	290.8	290.8	294.2	296.3	294.2	296.3	294.2		294.2				
8	292.8	292.8	298.3	296.3		298.3	301.8	296.3	297.6		295.6			290.8
7	286.6	295.6	292.8	295.6	297.6	299.7			294.9				298.3	
6	292.1	292.8	291.4	298.3	295.6	295.6	295.6	291.4		291.4		303.2		
5	292.1	297.6	296.3	294.9	300.4	299.0	295.6	296.3			298.3			
4	290.1	294.2	293.5	295.6	299.0	298.3	300.4			290.1				
3	287.3	294.9	298.3	294.2	300.4	294.2		294.9				296.3	293.5	
2	287.3	298.3	295.6	295.6	293.5	299.0	291.4	293.5			308.7			294.2
1	282.5	283.9	297.6	300.4	300.4	298.3			282.5	294.9				

Bottom Section Results for Mat D

(a)

≤ 254.9
255 – 275.9
276 – 295.9
296-316.9
≥ 317
Not Tested

(b)

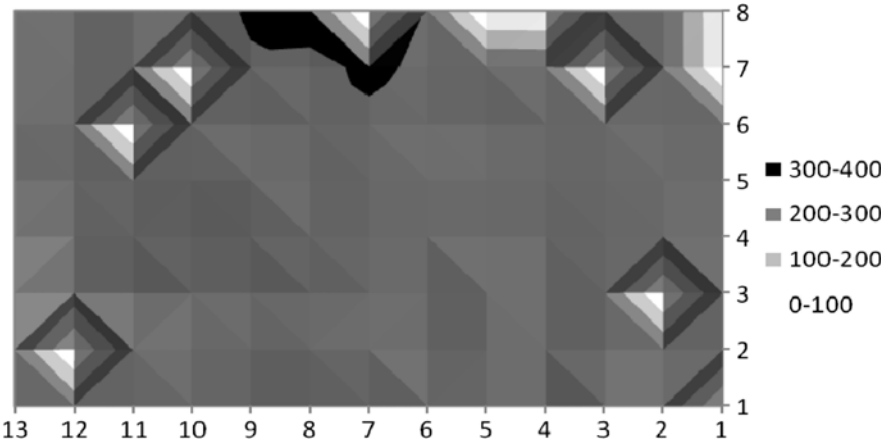

Fig. 6 (a) Yield strength of Mat D (measured in MPa). (b) Contour plot of yield strength of Mat D (MPa)

3.2 Mat D

Figure 6(a) shows the yield strength results of Mat D. Much like Mat C in Fig. 2(a), the light areas show a decrease in the properties of the mat in comparison to the remainder of the mat. The bottom of the mat appears to be affected as well, although not to the extent as that of the top. The most affected area of this mat (vertical lines) has an average value of 268 MPa (standard deviation of 5.9) which is above the minimum standard, 220.5 MPa (32 ksi). Again, a contour plot of these data is shown in Fig. 6(b).

The ultimate strength and hardness value results are similar to those of Mat C but slightly higher in values. The reason is that Mat D has less discoloration as compared to Mat C. Again the conductivity values are similar to Mat C and uniform in both the softer and harder areas. As a result, they could not be correlated with the color discoloration of the mat.

The 20 samples in the transverse direction were tested to determine their yield strength, ultimate strength, and hardness values. There was no significant difference (anisotropy) in testing in the transverse direction as compared to the longitudinal direction.

3.3 Percent Elongation

The percent elongation is not included in this article because many tensile samples broke outside the gauge length. Hardness measurements on both grips of these samples indicated that these samples broke adjacent to the grip of lower hardness. Optical microscopy on the grips indicated that the lower hardness grips had larger grains as compared to the grains of the higher hardness grips. These results are similar to those observed by Prietto et al. (Ref 6).

4. Discussion

A feasible solution to avoid the potential damage of the STOVL aircraft is to apply thermal coatings on them. Wilhelm et al. (Ref 2) studied the effect of eight different combinations of coatings, which were applied on the AM2 mats to evaluate which coating/s was/were best suited for use on mats exposed to exhaust from STOVL aircraft. Mats coated with NiAl bond coating, Al_2O_3-ZrO_2 heat resistance coating, and NiCr-SiC non-skid coating outperformed other coating combinations. Further testing was carried out on these coatings with varying thicknesses to optimize their performances (Ref 7).

5. Conclusions

Based on the investigation, we conclude that

1. The visible discolorations on the surfaces of the AM2 mats correlate to the drop in yield strength, ultimate tensile strength, and hardness. However, the electrical conductivity values remain the same.
2. The decreases in yield strength values are within the minimum AMS requirements.
3. The decreases in ultimate strength values in some portions are below the minimum AMS requirements, and the decreases in the hardness values are also below the typical values.

Acknowledgments

This study was funded by the National Science Foundation, NSF, Grant No. EEC-0353668, Research Experience for Undergraduate (REU) site.

References

1. N. Aizpuru, D. Le, J. McDonald, L. McLennan, S. Tewfik, E.W. Lee, D. Piatkowski, J. Foyos, J. Orgen, and O.S. Es-Said, The Effects of Flash Annealing on the Mechanical and Electrical Properties of Previously Used AM2 Mats Composed of Al 6061-T6, *Eng. Fail. Anal. J.*, 2005, **12**, p 691–698
2. C. Wilhelm, G. LaCaille, N. Wright, N. Ward, C. Shu, C. Vinquist, E. Lee, D. Piatkowski, J. McLennan, J. Ogren, and C. Kumor, Mechanical Properties and Microstructure Characterization of Coated AM2 Mats Exposed to Simulated Thermal Blast, *Eng. Fail. Anal. J.*, 2009, **16**, p 1–10
3. C. Maldonado, D. Diaz, J. Ranallo, R. Painter, W. Dahir, D. Hassouna, B. Gayer, E. Toss, I. Martinez, P. Stoyanov, J. Ogren, E.W. Lee, D. Piatkowski, J. Hilty, and O.S. Es-Said, Evaluation of the Effects of Powder Coating Cure Temperatures on the Mechanical Properties of Aluminum Alloy Substrates, *J. Mater. Eng. Perform.*, 2009, **18**(1), p 70–78
4. Aerospace Material Specifications, SAE AMS-QQ-A-250/11, 1997, p 3
5. Hardness and Conductivity Inspection of Wrought Aluminum Alloy Parts, AMS 2658, 2003
6. M. Prietto, M. Tsang, S. Hernandez, J. Roepke, D. Piatkowski, E. Lee, P. Stoyanov, J. Ogren, and O.S. Es-Said, The Effects of Heat Damage of Aluminum 6061-T6 AM-2 Mats and High Power Run-Up Anchor, submitted to *Eng. Fail. Anal. J.*, under review
7. C. Wilhelm, "Evaluation of AM2 Mats Thermal Barrier Coating Exposed to Simulated Vertical Take-Off and Landing Aircraft Engine Exhaust," M.S. thesis, Loyola Marymount University, Los Angeles, CA, 2008